AGU PUBLICATIONS

Water Resources Research

RESEARCH ARTICLE
10.1002/2017WR021592

Using High-Resolution Data to Assess Land Use Impact on Nitrate Dynamics in East African Tropical Montane Catchments

Suzanne R. Jacobs[1,2,3,4], Björn Weeser[3,5], Alphonce C. Guzha[6], Mariana C. Rufino[2,7], Klaus Butterbach-Bahl[1,4], David Windhorst[3], and Lutz Breuer[3,5]

[1]Karlsruhe Institute of Technology – Institute of Meteorology and Climate Research, Atmospheric Environmental Research (KIT/IMK-IFU), Garmisch-Partenkirchen, Germany, [2]Centre for International Forestry Research (CIFOR), Nairobi, Kenya, [3]Institute for Landscape Ecology and Resources Management (ILR), Justus Liebig University, Giessen, Germany, [4]Mazingira Centre, International Livestock Research Institute (ILRI), Nairobi, Kenya, [5]Centre for International Development and Environmental Research (ZEU), Justus Liebig University, Giessen, Germany, [6]US Forest Service – International Programs, Nairobi, Kenya, [7]Lancaster Environment Centre, Lancaster University, Lancaster, UK

Abstract Land use change alters nitrate (NO_3-N) dynamics in stream water by changing nitrogen cycling, nutrient inputs, uptake and hydrological flow paths. There is little empirical evidence of these processes for East Africa. We collected a unique 2 year high-resolution data set to assess the effects of land use (i.e., natural forest, smallholder agriculture and commercial tea plantations) on NO_3-N dynamics in three subcatchments within a headwater catchment in the Mau Forest Complex, Kenya's largest tropical montane forest. The natural forest subcatchment had the lowest NO_3-N concentrations (0.44 ± 0.043 mg N L^{-1}) with no seasonal variation. NO_3-N concentrations in the smallholder agriculture (1.09 ± 0.11 mg N L^{-1}) and tea plantation (2.13 ± 0.19 mg N L^{-1}) subcatchments closely followed discharge patterns, indicating mobilization of NO_3-N during the rainy seasons. Hysteresis patterns of rainfall events indicate a shift from subsurface flow in the natural forest to surface runoff in agricultural subcatchments. Distinct peaks in NO_3-N concentrations were observed during rainfall events after a longer dry period in the forest and tea subcatchments. The high-resolution data set enabled us to identify differences in NO_3-N transport of catchments under different land use, such as enhanced NO_3-N inputs to the stream during the rainy season and higher annual export in agricultural subcatchments (4.9 ± 0.3 to 12.0 ± 0.8 kg N ha^{-1} yr^{-1}) than in natural forest (2.6 ± 0.2 kg N ha^{-1} yr^{-1}). This emphasizes the usefulness of our monitoring approach to improve the understanding of land use effects on riverine N exports in tropical landscapes, but also the need to apply such methods in other regions.

Key Points:
- Catchments dominated by agricultural land use exported up to four times more nitrate than a forested catchment
- Hysteresis analysis showed a shift from subsurface flow to surface runoff in agricultural catchments during storm events
- Distinct peaks in nitrate concentrations in the forest and tea plantation subcatchments were observed during storms after a long dry period

Supporting Information:
- Supporting Information S1

Correspondence to:
M. C. Rufino,
m.rufino1@lancaster.ac.uk

Citation:
Jacobs, S. R., Weeser, B., Guzha, A. C., Rufino, M. C., Butterbach-Bahl, K., Windhorst, D., & Breuer, L. (2018). Using high-resolution data to assess land use impact on nitrate dynamics in East African Tropical Montane Catchments. *Water Resources Research*, *54*, 1812–1830. https://doi.org/10.1002/2017WR021592

Received 26 JUL 2017
Accepted 20 FEB 2018
Accepted article online 26 FEB 2018
Published online 12 MAR 2018

1. Introduction

Nitrogen (N) is a key element in terrestrial and aquatic ecosystems and plays an essential role in many biogeochemical processes, including primary productivity. Although organic N frequently constitutes a significant amount of total N export in temperate and tropical rivers (Alvarez-Cobelas et al., 2008; Gücker et al., 2016; Lewis et al., 1999), nitrate (NO_3-N) is more commonly studied due to its relative ease to measure compared to other forms of N, as well as its strong relation to human activity (Caraco & Cole, 1999). The latter makes it a suitable parameter to assess anthropogenic impacts on catchment water quality and biogeochemistry. The effect of land use on nutrient concentrations in tropical streams, and in particular NO_3-N, has been assessed in the past using spatial sampling campaigns (e.g., Biggs et al., 2004; Deegan et al., 2011; Gücker et al., 2016; Jacobs et al., 2017; Li et al., 2016), or low frequency monitoring of streams with contrasting land use (e.g., Lin et al., 2015; Neill et al., 2001; Ribeiro et al., 2014; Williams & Melack, 1997). Although such studies have provided valuable information on the potential effects of land use on nutrient concentrations, high-frequency long-term time series, facilitated by recent advances in *in situ* sensor technology, are required to obtain detailed information to quantify complex and highly responsive nutrient dynamics in streams (Blaen et al., 2016; Bowes et al., 2009; Burt, 2003; Kirchner et al., 2004; Rode et al., 2016).

In the case of NO_3-N, such high-frequency data have been used in temperate regions to improve load estimates (Ferrant et al., 2013; Fogle et al., 2003; Pellerin et al., 2014; Rozemeijer et al., 2010), to identify NO_3-N

sources (Bowes et al., 2015), to assess responses to rainfall events and hysteresis (Dupas et al., 2016; Lloyd et al., 2016b; Sherson et al., 2015), diurnal nutrient cycling patterns (Aubert & Breuer, 2016; Aubert et al., 2016; Halliday et al., 2012, 2013; Pellerin et al., 2009), responses to disturbances (Sherson et al., 2015), and nutrient dynamics in general (Bende-Michl et al., 2013; Halliday et al., 2012, 2013; Neal et al., 2012). Furthermore, *in situ* instruments can also be used to identify "hot moments" in nutrient concentrations and export. "Hot moments" are short periods with enhanced biogeochemical activity (McClain et al., 2003). Such short-lived events can be easily missed in monitoring programs based on grab sampling, but can still contribute significantly to total stream nutrient export. In contrast to temperate regions, there are very few examples in the tropics whereby *in situ* sensors for high-frequency measurements have been deployed (e.g., Waterloo et al., 2006; Zuijdgeest et al., 2016), and no such studies have been done in East Africa. The tropics generally receive less attention in water quality research compared to the temperate zone, yet tropical countries face higher rates of deforestation and land use change. Additionally, due to differences in climate, seasonality and soil types, which influence hydrological and biogeochemical processes, it is unlikely that knowledge obtained from temperate studies can directly be transferred to the tropics. Therefore, additional research is required to increase our understanding of the effect of land use change on water quality and discharge in tropical, and especially tropical montane regions, since these are generally key sources of fresh water (Bruijnzeel, 2001; Célleri & Feyen, 2009). Furthermore, understanding processes and dynamics of water and solutes, especially by comparing multiple catchments, is essential to increase our understanding of general catchment ecohydrology, which will improve our ability to model and predict nutrient dynamics and transport (Abbott et al., 2016).

The Sondu River is one of the twelve major rivers originating in the Mau Forest Complex, Kenya's largest remaining tropical montane forest and a water source for about 5 million people (UNEP et al., 2008). The forest is under significant human pressure through encroachment of smallholder farms, illegal tree logging, charcoal burning and grazing, which resulted in a 25% forest loss between 1973 and 2013 (Kinyanjui, 2011; Swart, 2016). Additionally, part of the area has been converted to commercial tea plantations during the 20th century. These changes have led to differences in soil hydraulic properties (Owuor et al., 2018), likely affecting NO_3-N inputs to the stream through changes in flow paths, like increased surface runoff, also referred to as overland flow (Mitchell, 2001). Intensive use of fertilizers specifically by commercial tea plantations, could have led to increased NO_3-N concentrations in the soil, leaching and subsequent subsurface flow to the stream, depending on the connectivity of the NO_3-N store to the stream (Musolff et al., 2015). Differences in soil C and N stocks as well as gaseous N losses observed for the different land use types in the area by Arias-Navarro et al. (2017) and Chiti et al. (2017) suggest that land use has strongly affected biogeochemical processes. Moreover, these studies indicate that land use change modified the dynamics of soil organic N and C decomposition, nitrification and denitrification, and soil temperature, soil pH and soil aeration.

The objective of this study was to understand the processes driving stream water NO_3-N dynamics in this tropical montane ecosystem and how these dynamics are affected by land use. We used a 2 year high-resolution data set from three subcatchments (27–36 km^2) dominated by either natural forest, smallholder agriculture or commercial tea and tree plantations to investigate: (a) seasonal patterns in stream water NO_3-N concentration and loading, (b) solubility, reactivity and source dynamics of NO_3-N through assessment of concentration-discharge relationships (Moatar et al., 2017; Musolff et al., 2015), (c) flow paths and NO_3-N sources through the analysis of responses to storm events (Dupas et al., 2016; Evans & Davies, 1998), and (d) occurrence of "hot moments" in NO_3-N concentrations and export. We compared the patterns for the subcatchments to those observed downstream at the outlet of the main catchment (1,021 km^2), to estimate how NO_3-N responses to land use are reflected at a larger scale. We hypothesized that groundwater is the main source of NO_3-N in stream water and, consequently, that leaching of fertilizer inputs lead to increased NO_3-N concentrations and loads in the tea plantations and smallholder agriculture subcatchments. Furthermore, we hypothesized that surface runoff occurs more frequently in nonforested catchments, resulting in dilution of NO_3-N concentrations during rainfall events.

2. Methods

2.1. Study Area

This study focuses on the catchment of the Chemosit River in the South-West Mau, a tributary of the Sondu River, which drains into Lake Victoria (Figure 1). The elevation in the Chemosit catchment ranges from

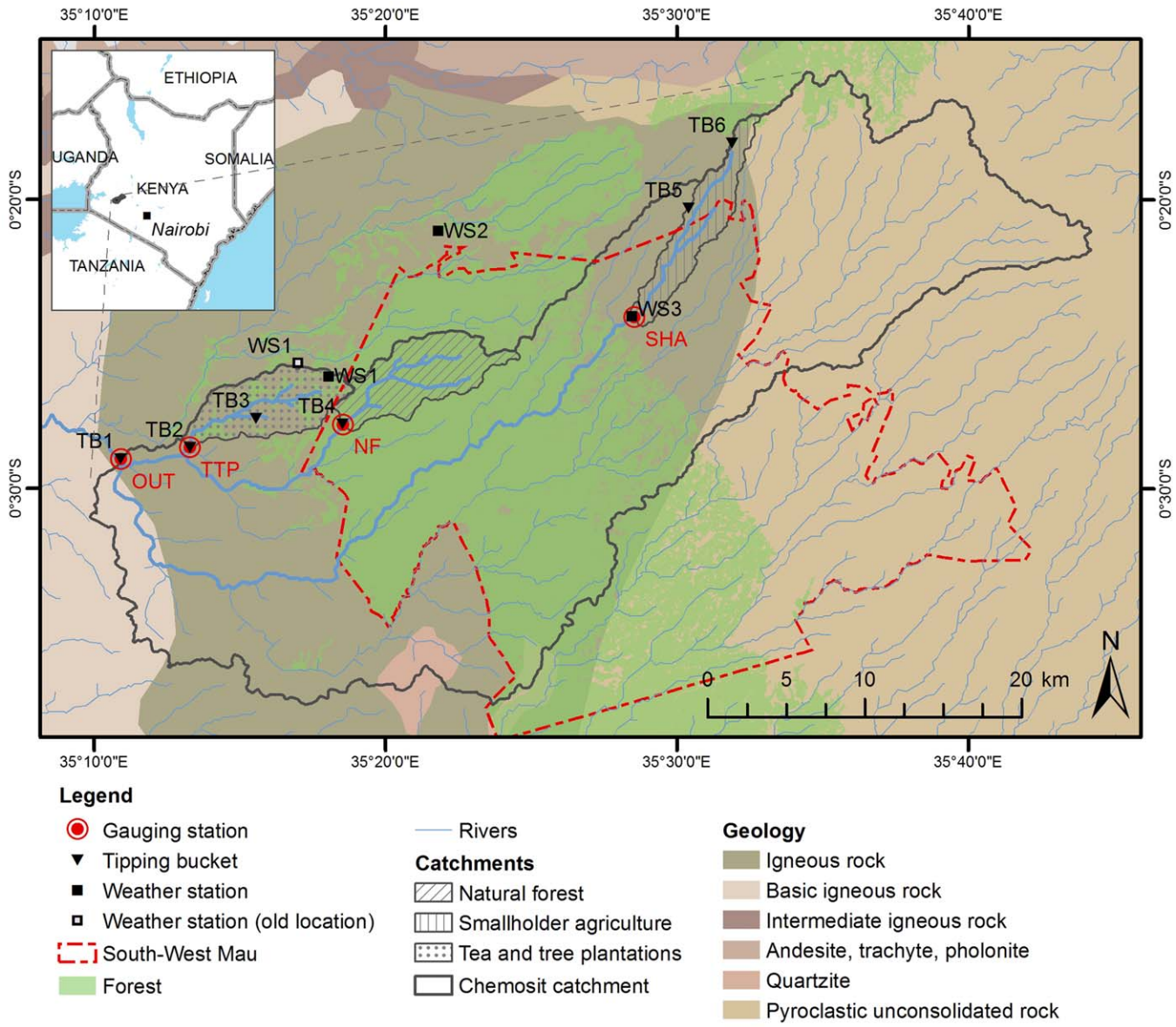

Figure 1. Map of the study area, geology and location of the automatic measurement systems (OUT = main outlet, TTP = commercial tea and tree plantations, NF = natural forest, SHA = smallholder agriculture), tipping buckets (TB1–6) and weather stations (WS1–3) in the South-West Mau, Kenya. Monitored rivers indicated with bold lines join at the main outlet (OUT). Geology data are from the Soil and Terrain database for Kenya (KENSOTER) version 2.0 (ISRIC, 2007).

2,932 m on top of the Mau Escarpment to 1,715 m at the outlet. The landscape is characterized by three main land use types: natural forest (NF), smallholder agriculture (SHA) and commercial tea and tree plantations (TTP). The upper part of the catchment, above 2,400 m elevation, is dominated by smallholder agriculture. Farmers grow maize, beans, potatoes and cabbage on plots of less than 2 ha. Fertilizer application rates are usually below 20 kg N ha^{-1} yr^{-1}. Crop fields are alternated with pastures for cattle grazing and woodlots of Eucalyptus, Cypress and Pine. In most places the riparian zones are severely degraded.

Natural forest vegetation is mainly found between 1,900 and 2,400 m elevation and is classified as Afromontane mixed forest (Kinyanjui, 2011), changing to montane bamboo forest above 2,300 m. At lower elevation, the landscape is dominated by smallholder farms in the south and by commercial tea plantations in the west. The latter consist of a mosaic of tea fields and Eucalyptus and Cypress plantations to supply the tea factories with fuel wood and timber. Riparian forest strips of up to 30 m width within the commercial tea

Table 1
Characteristics and Precipitation[a] Data of the Three Subcatchments and the Main Catchment in the South-West Mau, Kenya

Catchment	Area (km^2)	Elevation (m)	Mean ± SD slope (%)	Precipitation 2015 ($mm\ yr^{-1}$)	Precipitation 2016 ($mm\ yr^{-1}$)
Natural forest (NF)	35.9	1,954–2,385	15.5 ± 8.0	2,034	1,895
Smallholder agriculture (SHA)	27.2	2,380–2,691	11.5 ± 6.5	1,630	1,373
Tea/tree plantations (TTP)	33.3	1,786–2,141	12.2 ± 7.3	1,934	1,667
Main catchment (OUT)	1,021.3	1,715–2,932	12.8 ± 7.7	1,832	1,648

[a]Annual precipitation for 2015 and 2016 is based on data from six tipping buckets and three weather stations across the main catchment as indicated in Figure 1.

plantations are well maintained. Fertilizer is applied to tea fields by airplane in pellet form at 150–250 kg N $ha^{-1}\ yr^{-1}$ depending on crop demand.

Geology is fairly similar throughout the catchment, with phonolitic nephelinites dominating the upper part of the catchment with a variety of Tertiary tuffs (Jennings, 1971), whereas the lower part is characterized by phonolites (Binge, 1962). Soils are classified as humic Nitisols (ISRIC, 2007). The long-term (1905–2014) annual rainfall is 1988 ± 328 mm at 2,100 m elevation (Jacobs et al., 2017). Most of the rain falls between April and July (long rainy season) and between October and December (short rainy season). January to March are the driest months. Catchment characteristics and annual precipitation during the study period are shown in Table 1. A more detailed description of the study area can be found in Jacobs et al. (2017).

2.2. Instrumentation

2.2.1. Automatic Measurement Systems

We used a nested approach, whereby three subcatchments of 27–36 km^2 were selected within the Chemosit catchment, based on (a) dominant land use, (b) comparability of geological substrate, (c) security of equipment, and (d) accessibility (Table 1 and Figure 1). The identified sites, i.e., the natural forest (NF), smallholder agriculture (SHA) and tea and tree plantation (TTP) subcatchments, were instrumented with an automatic measurement system at the start of the short rainy season in October 2014. The outlet of Chemosit catchment, from now on referred to as the main catchment (OUT), was instrumented at the end of the dry season in April 2015.

Each automatic system recorded water level with a radar-based sensor (VEGAPULS WL61, VEGA Grieshaber KG, Schiltach, Germany) with a resolution of < 1 mm and a measurement accuracy < 2 mm. Water level data were complemented with regular discharge measurements using the salt dilution method with slug injection (Moore, 2004), an Acoustic Doppler Velocimeter (ADV; FlowTracker, SonTek, San Diego CA, USA) or an Acoustic Doppler Current Profiler (ADCP; RiverSurveyor S5, SonTek, San Diego CA, USA) depending on river size and discharge to develop a rating curve (see section 2.4.1). Nitrate (NO_3-N) concentrations were measured *in situ* using UV/Vis spectroscopy (spectro::lyser, s::can Messtechnik GmbH, Vienna, Austria). NO_3-N data were calibrated using reference grab samples (see section 2.2.2). To reduce the influence of sediment and debris, the submerged sensors were cleaned automatically with a pulse of compressed air before each measurement. Although the cleaning system greatly reduced sedimentation on the sensor windows, additional weekly manual cleaning was necessary to remove biofouling. The instruments ran on solar power and measured all parameters at a 10 min interval.

2.2.2. Reference Grab Samples and Calibration

Weekly or bi-weekly reference stream water samples were taken from all sites for calibration. Flow conditions during sampling covered 71 to 82% of the observed discharge range, missing high flows during storm events. Samples were drawn from the stream using a 60 ml syringe pre-rinsed with stream water. The water was then filtered through a 0.45 μm polypropylene filter (Whatman Puradisc 25 syringe filter, GE Healthcare, Little Chalfont, UK or KX syringe filter, Kinesis Ltd., St. Neods, UK) and collected in clean 100 ml HDPE bottles. The bottles were transported in a cooler box with ice and frozen at −20°C until final analysis for NO_3-N using ion chromatography (ICS-2000, Dionex, Sunnyvale CA, USA) and total dissolved nitrogen (TDN; TOC cube, Elementar Analysensysteme GmbH, Hanau, Germany) in the laboratory of Justus Liebig University

Giessen, Germany. A linear regression model between field and laboratory measurements was used for calibration of the field data for each site.

2.2.3. Rainfall Data

Rainfall was measured with tipping buckets at nine locations (TB1–6: Theodor Friedrichs, Schenefeld, Germany, and WS1–3: ECRN-100 high resolution rain gauge, Decagon Devices, Pullman WA, USA; Figure 1), recording cumulative rainfall every 10 min. WS1 had to be relocated in September 2015 due to construction activities on site. For each catchment, rainfall was calculated by weighting the data from relevant tipping buckets using Thiessen polygons. Weights were adjusted when data were missing due to funnel blockage or instrument malfunctioning, omitting the tipping buckets for which no data were available (NF = 50.0%, SHA = 17.7%, TTP = 19.5% and OUT = 34.9% of time).

2.3. Data Processing

2.3.1. Flagging Unreliable Data

A protocol was set up for the processing of all data collected by the automatic stations to ensure reproducibility (supporting information Figure S1). Unique flags differentiated reasons for classifying a measurement as unreliable (supporting information Table S1). The flags were categorized as (a) automated, when allocated automatically using a R script (R Core Team, 2015), or (b) manual, when assigned based on log book information and field observations. A third group of flags (calculation) was added to identify measurements that were adjusted, calibrated or calculated during post-processing. In total, 4.1–7.4% and 0.1–0.4% of the data were flagged as unreliable for NO_3-N and water level, respectively (supporting information Figure S1).

2.3.2. Biofouling Correction

On occasions where the automatic cleaning system failed, biofouling on the windows affected measurements by the spectro::lyser. Laboratory analyses confirmed that the measurement following manual cleaning represented the expected stream water NO_3-N concentration. These data were used to calculate a build-up rate of biofouling (0.02–0.19 mg L^{-1} d^{-1}) and to correct the measurements during periods of cleaning system failure. Correction was necessary on one occasion for OUT (7 days) and six occasions (3–10 days) for TTP.

2.3.3. Outlier Detection

A robust tool for outlier detection is the median absolute deviation (MAD):

$$MAD_i = b\ M_{i2}(|x_i - M_{i1}(x_i)|) \tag{1}$$

where x_i is the data set for which the MAD is calculated, M_{i1} the median of data set x_i and M_{i2} the median of the absolute deviation of the data set from its median. Consistency constant b is included to create a robust estimator for the estimation of the standard deviation and is set to 1.4826 for a normal distribution (Leys et al., 2013).

To detect local outliers, we applied a moving window of k measurements around observation x_i at time t_i. The $MAD_{j,i}$ was calculated for observations $x_j = (x_{i-k/2}...x_{i-1}, x_{i+1}...x_{i+k/2})$. Measurement x_i was flagged as outlier if:

$$\left|\frac{x_i - M_{j,i}}{MAD_{j,i}}\right| > a \tag{2}$$

where a is the threshold for outlier selection, and $M_{j,i}$ and $MAD_{j,i}$ are the median and MAD of x_j. Because the aim was to flag values with large deviation from the remaining data set, a conservative value of $a = 6$ was selected. The value of $k = 16$ was selected based on multiple runs with different values for a and k for NO_3-N and water level data. Outlier detection was carried out after omitting data flagged as unreliable in previous processing steps, as these data could confound the identification of potential outliers.

2.4. Data Analysis

2.4.1. Discharge Calculation

We developed a rating curve (second order polynomial; supporting information Figure S2) for each catchment using discharge measurements taken at each site over a wide range of water levels, which was then applied to the water level data to estimate discharge. The same polynomial function was used for extrapolation above the highest measured discharge, while extrapolation below the lowest measured discharge was done using a quadratic function through the lowest measured discharge and zero discharge. The rating

curves were checked after their establishment by frequent discharge measurements at each site. Discharge was converted to specific discharge ($Q_{s,i}$), also referred to as specific runoff, in mm d^{-1}.

2.4.2. Load Calculation

NO_3-N concentrations and discharge were used to calculate loads for the three subcatchments for 2015 and 2016. For the main catchment loads were only calculated for 2016, because measurements at this site started end of April 2015. Linear interpolation was applied in gaps of $\leq$ 24 h in the 10-min time series data of NO_3-N (0.78–1.22% of data; supporting information Table S2). Interpolation for gaps $>$ 24 h (2.82–9.45% of data) was done using a smoothed data set to minimize the influence of within-day NO_3-N variation due to rainfall events and diurnal cycling at the start and end of the data gap. For smoothing, a rolling median with a 48 h window width was selected to minimize the influence of outliers. Additionally, manual grab samples were used to interpolate data gaps. The final data set consisted of all points for which both discharge and (estimated) NO_3-N concentration was available. Load (L_i) in g s^{-1} at time t_i was calculated using:

$$L_i = C_i Q_i \tag{3}$$

where C_i is the NO_3-N concentration in mg N L^{-1} and Q_i is discharge in m^3 s^{-1} at time t_i. Specific load ($L_{s,y}$) in kg ha^{-1} yr^{-1} in year y was calculated with:

$$L_{s,y} = K_2 \sum_{i=1}^{n} \left(\frac{L_i}{A} \Delta t_i \right) \tag{4}$$

where A is catchment area in ha, Δt_i the time interval for the observation in seconds and n the total number of observations. Constant $K_2 = 10^{-3}$ was applied to convert units from g ha^{-1} yr^{-1} to kg ha^{-1} yr^{-1}.

2.4.3. Uncertainty Estimation

A 95% confidence interval (CI) for the linear relationship between field and laboratory measurements was used to estimate uncertainty in NO_3-N concentration. This approach considers the uncertainty in the laboratory measurements to be negligible, and treats the spectro::lyser measurements as the primary source of uncertainty. For uncertainty in discharge, we estimated the uncertainty in individual discharge and water level measurements for the rating curve based on the standard deviation (SD) of repeated measurements. Assuming that the size of the SD increases proportionally to the discharge, the SD for salt dilution measurements was 6.9%, while ADV and ADCP measurements had a SD of 4.2 and 6.2% respectively. Water level measurements had a SD of 1.0 mm. Following the procedure of McMillan et al. (2010), we assumed that the true discharge or water level value was within 3*SD from the measured value. For each combination of water level and discharge on the rating curve, 10,000 random samples within the 3*SD uncertainty limit of water level and discharge were taken and rating curves were generated for each set of samples. The 95% CI was calculated using the empirical cumulative distribution function for discharge estimated with all 10,000 simulated rating curves.

For NO_3-N load, uncertainties in discharge and NO_3-N concentration were included:

$$\frac{\varepsilon_L}{L} = \sqrt{\left(\frac{\varepsilon_C}{C}\right)^2 + \left(\frac{\varepsilon_Q}{Q}\right)^2} \tag{5}$$

where ε_L is the uncertainty in the load, ε_C in concentration, and ε_Q the uncertainty in discharge.

2.4.4. Hysteresis Analysis

Ten storm events were selected to study the response of NO_3-N concentrations to changes in discharge due to rainfall. The events represented five different periods in the year: dry season (DS), start of the long rainy season (SLR), long rainy season (LR), period of moderate rainfall between the long and short rainy season (MR) and the short rainy season (SR). Event dates were chosen based on occurrence of rainfall events in all catchments in that period and a minimum 30% increase in discharge during the event in each subcatchment. No data were available for the dry season event in 2015 for TTP and OUT. Hysteresis patterns were assessed using plots of normalized discharge and NO_3-N concentrations:

$$P_{norm,i} = \frac{P_i - P_{\min}}{P_{\max} - P_{\min}} \tag{6}$$

where $P_{norm,i}$ and P_i are the normalized and original value of the parameter at time t_i, and P_{min} and P_{max} are the minimum and maximum observed values during the event. In addition to visual assessments of

hysteresis patterns and direction of hysteresis loops, we calculated the hysteresis index (*HI*) as proposed by Lloyd et al. (2016a) for every 5th percentile of the normalized discharge of the storm event:

$$HI_i = C_{norm,r,i} - C_{norm,f,i} \quad (7)$$

where HI_i is the hysteresis index for percentile *i*, and $C_{norm,r,i}$ and $C_{norm,f,i}$ the normalized NO_3-N concentration on the rising and falling limb for the i^{th} percentile of normalized discharge, respectively. The mean *HI* of all percentiles was used to assess hysteresis of each storm event. Negative and positive mean *HI* generally indicate anti-clockwise and clockwise hysteresis loops, respectively. However, events with a mean *HI* close to zero usually have a more complex hysteresis pattern and are better interpreted visually. In addition to mean *HI*, a set of storm metrics was calculated to characterize each event: the antecedent precipitation index for 30 days before the event (API_{30}), total precipitation, rainfall intensity during the event, the antecedent concentration and discharge, and relative change in concentration and discharge.

3. Results

3.1. Specific Discharge

The specific discharge time series in the three subcatchments and main catchment clearly reflected the seasonality in rainfall. The highest discharge peaks were observed during the long rainy season from April to July in both years (Figure 2). High specific discharge was also observed during the short rainy season in November and December 2015, but not in 2016. Although mean specific discharge was significantly lower in the smallholder agriculture (SHA; 1.4 ± 1.2 mm d^{-1}) than in the natural forest (NF; 1.9 ± 1.7 mm d^{-1}) and commercial tea and tree plantation (TTP; 1.9 ± 1.8 mm d^{-1}) subcatchments ($p < 0.001$), TTP had the lowest median specific discharge (1.1 mm d^{-1}) compared NF (1.3 mm d^{-1}) and SHA (1.2 mm d^{-1}), and highest annual runoff coefficient (Table 2). The main catchment (OUT) had the highest median specific discharge (1.3 mm d^{-1}) and the temporal discharge pattern reflected the specific discharge patterns of the three subcatchments. Differences in rainfall patterns between the three subcatchments resulted in a different timing of peaks in specific discharge.

3.2. NO_3-N Concentrations

3.2.1. Relationship Between Field and Laboratory Measurements

There was a strong relationship between NO_3-N concentrations measured in the field and in the laboratory at all sites (Figure 3). TTP had the best linear model fit with $R^2 = 0.899$, whereas measurements at OUT had the poorest fit ($R^2 = 0.565$). Better fits were obtained for sites for which grab samples were taken over a larger range and slightly higher NO_3-N concentrations. The differences among sites could also be related to site-specific surface water properties, such as water temperature, turbidity and color that affect sensor performance. The sensor at the outlet of NF tended to overestimate NO_3-N concentrations at concentrations > 0.5 mg N L^{-1}, while the sensors at SHA and TTP slightly underestimated the concentrations. The maximum measured NO_3-N concentration at NF (2.27 mg N L^{-1}) was more than twice the maximum of the range of values used for calibration (0.99 mg N L^{-1}), but concentrations higher than 0.80 mg N L^{-1} occurred less than 1% of the time.

3.2.2. Temporal Variations in NO_3-N Concentrations

The flow-weighted mean NO_3-N concentration was lowest at NF (0.44 ± 0.043 mg N L^{-1}), followed by SHA (1.10 ± 0.11 mg N L^{-1}) and TTP (2.14 ± 0.19 mg N L^{-1}). The mean NO_3-N concentration at OUT (0.89 ± 0.10 mg N L^{-1}) was slightly lower than at SHA. NO_3-N concentrations at NF were mostly within a range of 0.3–0.5 mg N L^{-1} throughout the year (Figure 4). Conversely, concentrations in SHA, TTP and OUT showed a seasonal pattern with higher concentrations during periods of high flow. NO_3-N contributed most to total dissolved nitrogen (TDN) in all catchments, with 83 ± 32% in NF, 75 ± 16% in SHA, 83 ± 17% in TTP and 79 ± 16% in OUT.

3.2.3. Concentration-Discharge Relationship and Hysteresis

The concentration–discharge relationships differed for the subcatchments: NO_3-N concentrations at NF were not related to discharge ($R^2 = 0.070$), for SHA and TTP there were positive (log-linear) relationships ($R^2 = 0.630$ and $R^2 = 0.725$), whereas for OUT there was a weak positive (log-linear) relationship ($R^2 = 0.217$; Figure 5 and supporting information Figure S3).

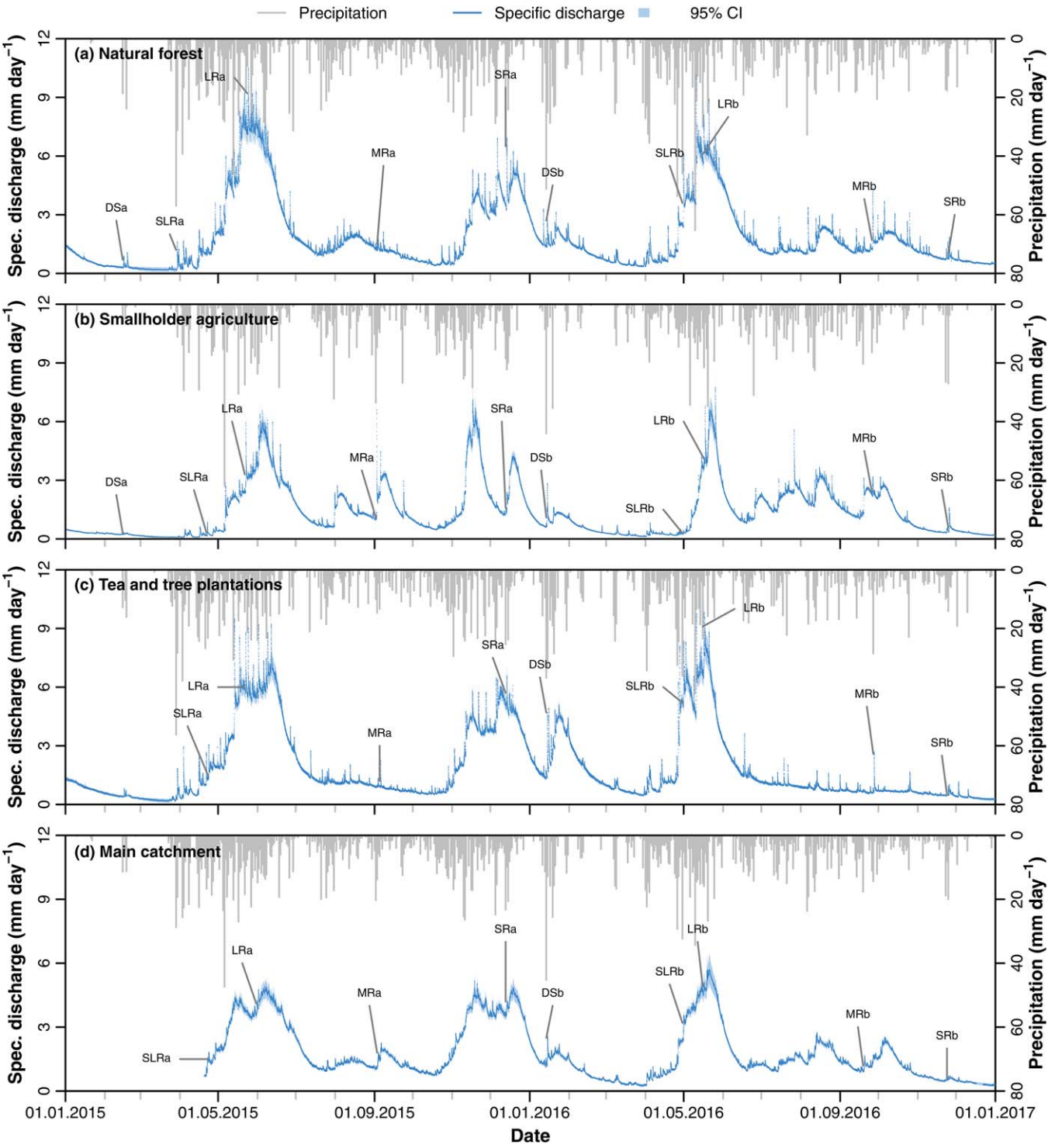

Figure 2. Precipitation and specific discharge time series with 95% confidence interval (CI) at the outlet of the (a) natural forest (NF), (b) smallholder agriculture (SHA), and (c) tea and tree plantation (TTP) subcatchments and (d) the main catchment (OUT) in the South-West Mau, Kenya, between January 2015 and December 2016. Labels indicate selected storm events for hysteresis analysis.

Normalized concentration–discharge graphs per rainfall event and catchment are provided in supporting information Figures S4 and S5. Most events at NF followed an anti-clockwise hysteresis loop indicated by negative mean hysteresis indices (*HI*; supporting information Table S3), with lower concentrations on the rising limb than on the falling limb of the hydrograph. Events during low flow showed the highest relative

Table 2
Annual Specific Discharge, Runoff Coefficient and Specific NO_3-N Load (and 95% Confidence Interval) for the Studied Catchments[a] in the South-West Mau, Kenya

Catchment	Year	Specific discharge (mm yr^{-1})	Runoff coefficient[b]	Specific NO_3-N load (kg N ha^{-1} yr^{-1})
NF	2015	724 (676–772)	0.36 (0.33–0.38)	3.23 (2.98–3.48)
	2016	609 (574–644)	0.32 (0.30–0.34)	2.62 (2.43–2.80)
SHA	2015	535 (500–571)	0.33 (0.31–0.35)	6.04 (5.58–6.49)
	2016	465 (437–493)	0.34 (0.32–0.36)	4.92 (4.57–5.26)
TTP	2015	744 (698–789)	0.38 (0.36–0.41)	16.26 (15.21–17.31)
	2016	582 (547–618)	0.35 (0.33–0.37)	12.04 (11.24–12.83)
OUT	2016	512 (477–547)	0.31 (0.29–0.33)	4.56 (4.12–5.00)

[a]NF = natural forest, SHA = smallholder agriculture, TTP = tea and tree plantations, OUT = main catchment. [b]Annual specific discharge as proportion of annual precipitation.

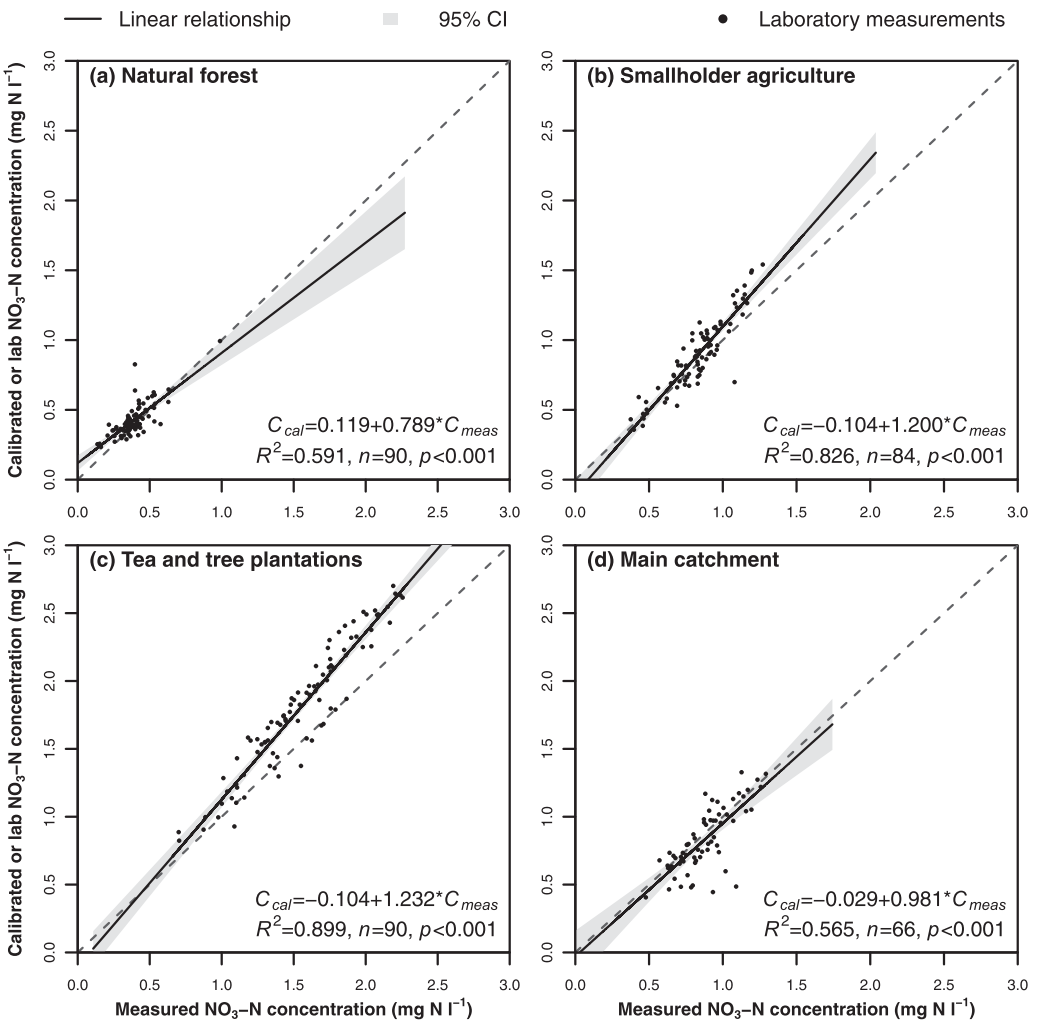

Figure 3. Linear relationship and the 95% confidence interval (CI) between measured and calibrated nitrate (NO_3-N) concentrations for the full range of concentrations measured in the field between January 2015 and December 2016 at each site, based on the relationship between values measured by the sensor in the field and as obtained through corresponding grab samples analyzed in the laboratory (black dots) for the (a) natural forest (NF), (b) smallholder agriculture (SHA) and (c) tea and tree plantations (TTP) subcatchments and (d) the main catchment (OUT) in the South-West Mau, Kenya. The dashed line represents the 1:1 relationship between measured and calibrated values.

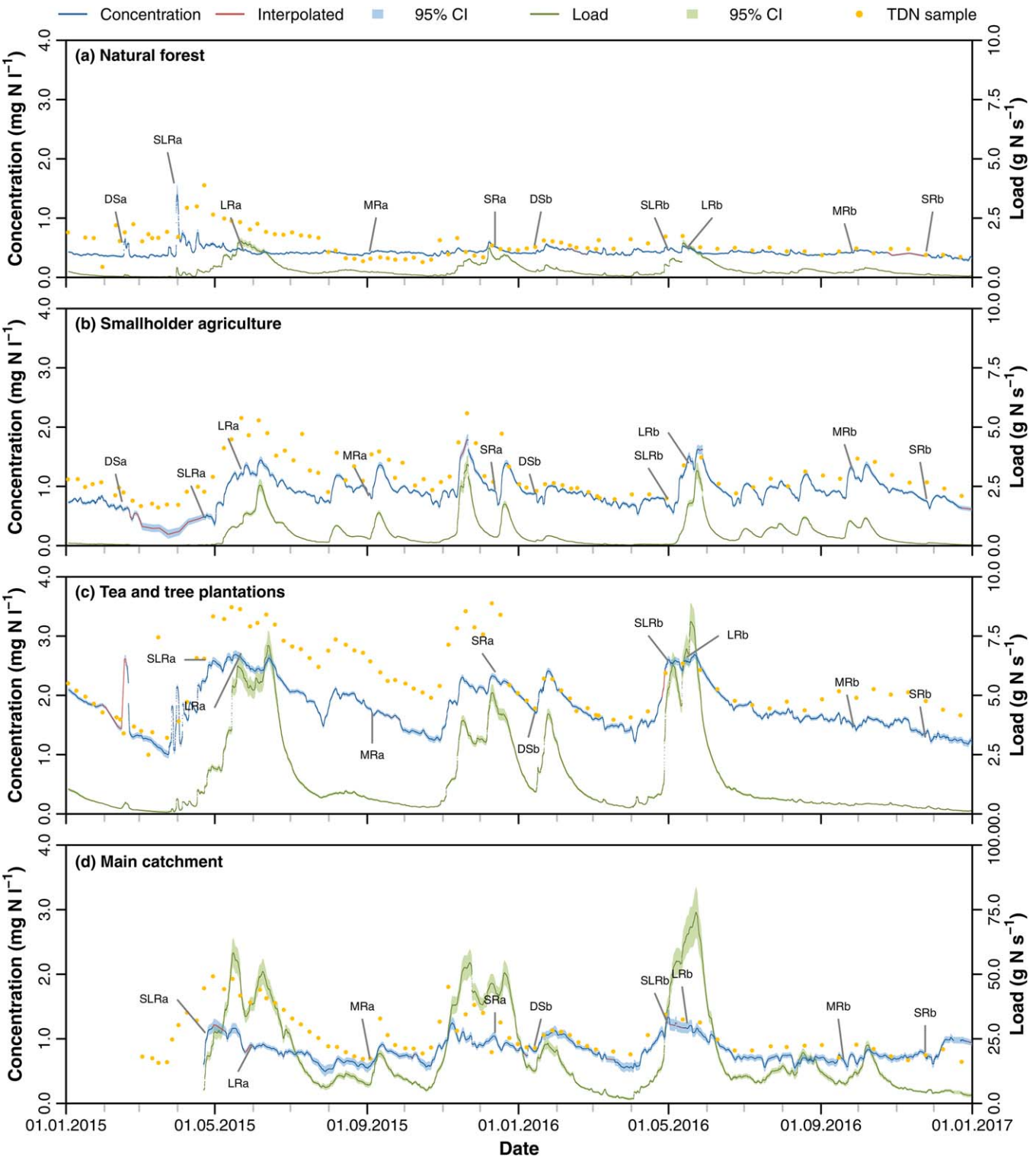

Figure 4. Time series of smoothed (48 h rolling median) nitrate (NO_3-N) concentration and loads with 95% confidence interval (CI), and TDN concentration at the outlet of the (a) natural forest (NF), (b) smallholder agriculture (SHA) and (c) tea and tree plantations (TTP) subcatchments and (d) the main catchment (OUT) in the South-West Mau, Kenya, between January 2015 and December 2016. Labels indicate selected storm events for hysteresis analysis.

increases in NO_3-N concentrations (up to 4-fold). The majority of events in SHA displayed a clockwise hysteresis loop with strong dilution on the falling limb of the hydrograph. Exceptions were event DSa and SLRa, both during or at the end of the low flow period, with an anti-clockwise loop or no clear pattern.

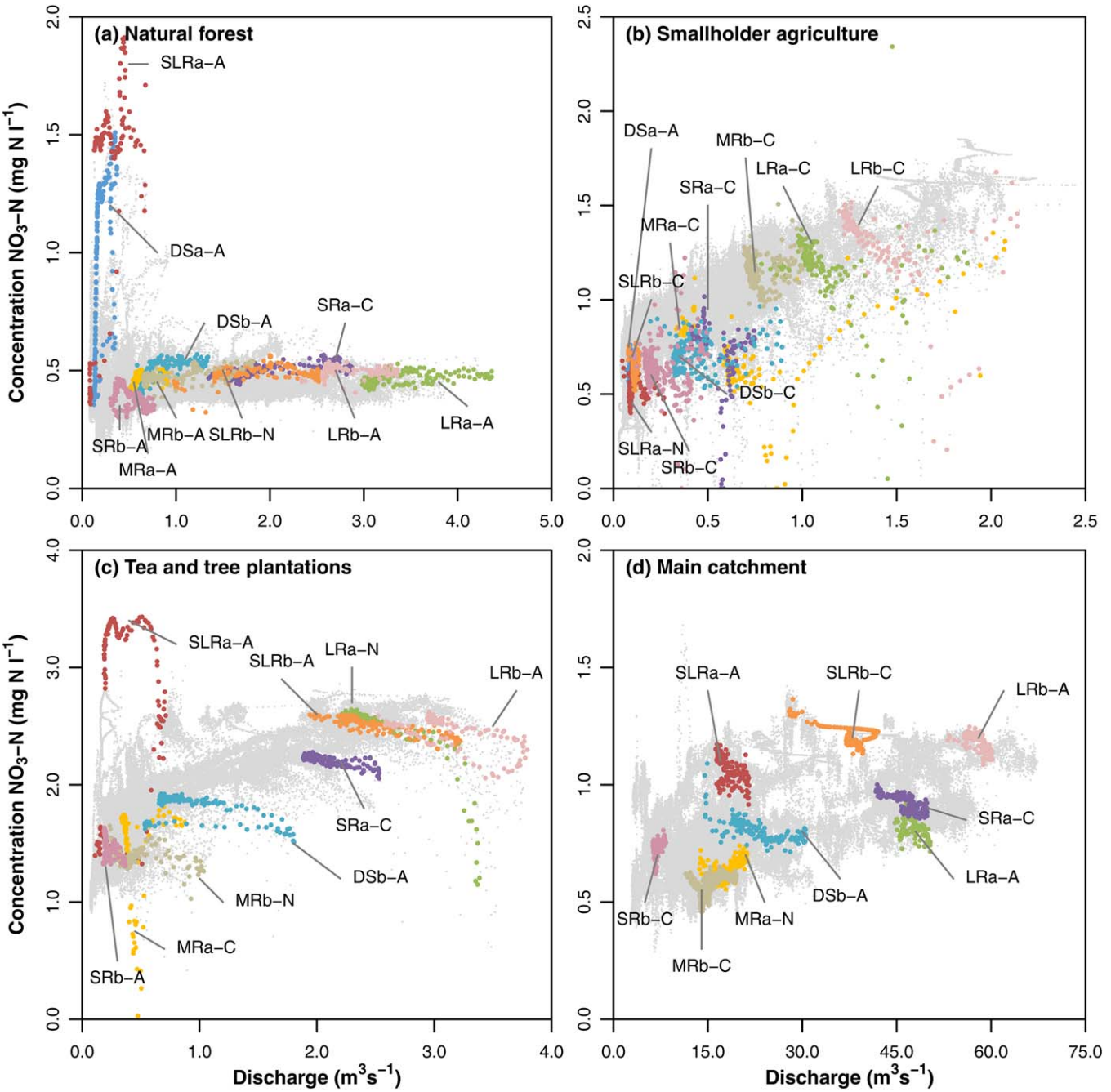

Figure 5. Discharge and nitrate (NO_3-N) concentration at the outlet of the (a) natural forest (NF), (b) smallholder agriculture (SHA), and (c) tea and tree plantations (TTP) subcatchment, and (d) the main catchment (OUT) in the South-West Mau, Kenya, measured between January 2015 and December 2016. The full data set is represented by grey dots. Selected storm events for hysteresis analysis are indicated by different colors and labels: DS = dry season, SLR = start long rainy season, LR = long rainy season, MR = moderate rainfall between long and short rainy season, and SR = short rainy season), year (a = 2015, b = 2016) and direction of hysteresis loop (A = anti-clockwise, C = clockwise, N = no loop). Labels correspond to the indicated storm events in Figure 2 and Figure 4.

Hysteresis patterns were less consistent for TTP and OUT. Although events in OUT showed anti-clockwise hysteresis loops during the long rainy season and clockwise loops during medium rainfall and the short rainy season, no systematic seasonal changes were observed for TTP. In TTP, larger storm events (high total precipitation and rainfall intensity) usually resulted in lower *HI*, but this was not observed for the other catchments. Similar to NF, event SLRa showed an anti-clockwise hysteresis loop with large increase in NO_3-N concentration in TTP. Most other events in TTP resulted in dilution of the NO_3-N concentration at the

peak of the hydrograph. Events with API_{30}>250 mm, mainly coinciding with the long rains, had a *HI* close to or below zero in all catchments. Also events at the start of the long rainy season generally displayed anticlockwise hysteresis loops ($HI < 0$), whereas storms during the short rains often showed a clockwise loop ($HI > 0$).

3.3. NO_3-N Loads

Loads in all catchments followed discharge patterns (Figure 4). The strong relationship between NO_3-N concentration and discharge in SHA and TTP (Figure 5 and supporting information Figure S3), resulted in pronounced seasonal peaks in NO_3-N loadings. Annual specific loads were more than four times higher in TTP than in NF, while loads for SHA were approximately twice those of NF (Table 2). The annual specific load of OUT was similar to that of SHA in 2016. All catchments exported less NO_3-N in 2016 than in 2015.

4. Discussion

4.1. Seasonal NO_3-N Patterns

There was no seasonal pattern in NO_3-N concentrations for the natural forest (NF), while NO_3-N concentrations in the smallholder agriculture (SHA) and commercial tea and tree plantations (TTP) followed a seasonal pattern with higher concentrations in periods of high discharge. Small, short-lived peaks ($<$ 0.2 mg N L^{-1} on top of baseline concentrations) in NO_3-N concentrations during storm events were observed during fertilizer application within TTP, likely as a result of surface runoff. However, the contribution of these peaks to the generally higher NO_3-N concentrations in TTP was very small and the gradual change in NO_3-N concentration during the rainy seasons in TTP and SHA was most likely a consequence of slower transport of NO_3-N to the stream through subsurface flow paths, as illustrated in Figure 6. NO_3-N retention in soils is related to the anion exchange capacity, which depends on mineralogy, soil pH, soil organic carbon (Harmand et al., 2010; Soares et al., 2005) and hydrological properties due to soil age and development (Lohse & Matson, 2005). Although the high kaolinite content of Nitisols, the dominant soil type in the study area, could contribute to NO_3-N retention (Harmand et al., 2010), the relatively high soil organic carbon content of the topsoil (58–97 g kg^{-1}) (Arias-Navarro et al., 2017) and well-drained soils in the study area could facilitate leaching of NO_3-N from the topsoil to groundwater during the rainy season (Rasiah et al., 2003). Increased NO_3-N input to the streams could also occur when discharge is produced directly from lateral flow through a NO_3-N rich soil layer (Musolff et al., 2015). During dry periods, this NO_3-N source is likely disconnected from the stream, thus resulting in lower concentrations during periods of low rainfall. The upward shape of the concentration–discharge relationships of SHA and TTP confirms this chemodynamic behavior (Moatar et al., 2017). A spatially dynamic change in the discharge generating zone has also been observed for other tropical montane ecosystems, such as the Páramo in Ecuador (Correa et al., 2017). Therefore, it is likely that NO_3-N enters the stream via groundwater, a typical pathway discussed for many agricultural catchments (Durand et al., 2011). To further support this hypothesis groundwater measurements are needed, which are currently not available for our study catchments.

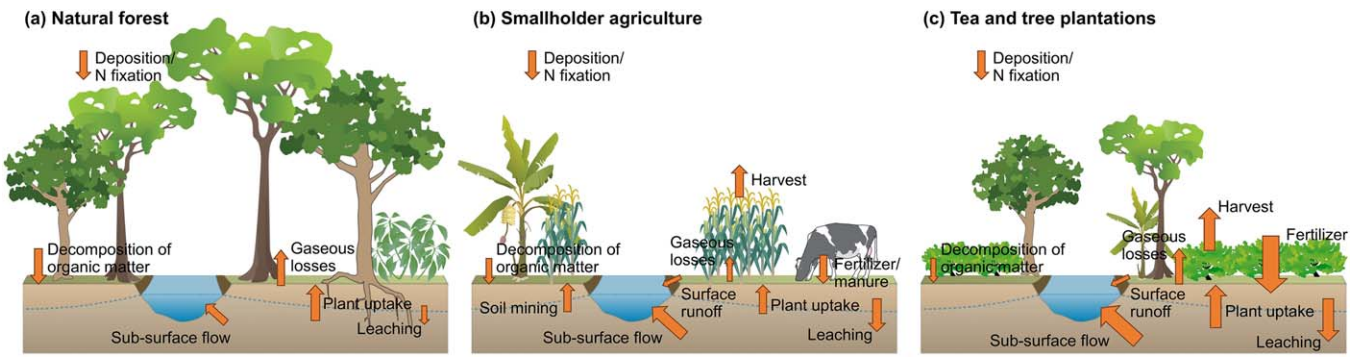

Figure 6. Conceptual model of nitrogen (N) fluxes in three land use types in a tropical montane area: (a) natural forest (NF), (b) smallholder agriculture (SHA) and (c) commercial tea and tree plantations (TTP), based on interpretation of the results of this study in the South-West Mau, Kenya. Differences in arrow size indicate relative differences in magnitude of fluxes between the three land use types.

The lack of seasonality in NO_3-N concentrations in NF is reflected in the absence of a relationship between concentration and discharge. This suggests chemostatic behavior, which could be caused by a uniform distribution of NO_3-N in the soil, continuous hydrological connectivity and temporal stability of flow paths (Moatar et al., 2017; Musolff et al., 2015). Furthermore, unlike SHA and TTP, which receive mainly organic and a significant amount of inorganic fertilizer, respectively, NF does not receive anthropogenic N inputs that accumulate in the soil and are mobilized during the rainy season. Although accumulation of NO_3-N in tropical forests has also been observed, mostly due to nitrification during the dry season (e.g., Kiese et al., 2003), this effect is usually confined to the topsoil and might not result in significant leaching losses. Chaves et al. (2009) reported NO_3-N concentrations two orders of magnitude higher in soil water at 20 cm depth than in groundwater in a tropical forest in the Amazon. They attributed this reduction along the vertical flow path to uptake by deep-rooted vegetation, denitrification and abiotic N retention in deeper soil layers, which was also observed by Harmand et al. (2010). These processes were also held responsible for a lack of seasonal in-stream NO_3-N variation despite increased NO_3-N concentrations in the upland and riparian zone in a tropical montane forest catchment in Peru (Saunders et al., 2006). However, because of differences between our study area and the aforementioned studies in soil type (e.g., Chaves et al., 2009), topography and soil depth (e.g., Saunders et al., 2006) and annual precipitation and temperature (e.g., Harmand et al., 2010) we cannot reliably conclude that the same processes are responsible for the observed patterns in our study without further empirical evidence.

4.2. Response to Storm Events

Hysteresis occurs when the timing or form of response of the solute concentration and discharge differ, generally resulting in a cyclical relationship between concentration and discharge (Evans & Davies, 1998). These hysteresis loops can be either clockwise, with higher concentrations on the rising limb of the hydrograph, or anti-clockwise, with higher concentrations on the falling limb. The direction and shape of the hysteresis loop reflects the timing of changes in concentration and discharge, as well as mixing processes, and allows interpretation of sources of stormflow and NO_3-N (Evans & Davies, 1998).

The anti-clockwise hysteresis loops with slight increases in NO_3-N concentrations at NF suggest slow mobilization of NO_3-N in top soil during storm events (Van Herpe & Troch, 2000), which has been observed in a Peruvian tropical montane forest (Saunders et al., 2006). According to a classification of hysteresis loops by Evans and Davies (1998) based on a three component mixing model with soil water, groundwater and surface runoff, the shape of most hysteresis loops in NF suggests inflow of NO_3-N rich soil water to the stream during the storm event. Large rainfall events ($>$ 30 mm) during wet periods ($API_{30} > 200$ mm; SRa and SLRb) showed no clear hysteresis loop and the NO_3-N concentration barely changed during the storm event. This suggests that antecedent moisture conditions and event size affect NO_3-N mobilization in NF, resulting in different hysteresis patterns.

The decrease in NO_3-N concentrations during storm events in TTP and SHA implies dilution of stream water with precipitation which is low in NO_3-N (0.20 ± 0.10 mg N L^{-1}, $n = 13$). This agrees with findings of Goodridge and Melack (2012), where agricultural catchments showed dilution during rainfall events, compared to NO_3-N enrichment in undisturbed catchments. Dilution of NO_3-N due to surface runoff was also observed in a subtropical agricultural catchment in Japan (Blanco et al., 2010) and a tropical agricultural catchment in the Amazon (Riskin et al., 2017). These results strongly indicate that conversion from natural forest to agricultural land use causes a shift from subsurface flow to surface runoff during storm events. The generally lower infiltration rates in SHA (40.5 ± 21.5 cm h^{-1} in croplands and 13.8 ± 14.6 cm h^{-1} in pastures) and TTP (43.3 ± 29.2 cm h^{-1} and 60.2 ± 47.9 cm h^{-1} in tea and tree plantations, respectively) than in NF (76.1 ± 50.0 cm h^{-1}), as presented by Owuor et al. (2018), could explain increased surface runoff across agricultural land during storm events. The concave shape and negative direction of the hysteresis loops further suggest that groundwater has higher concentrations than event and soil water (Evans & Davies, 1998), which supports our findings that groundwater enriched through leaching of NO_3-N from fertilizer inputs is the main source of increased NO_3-N concentrations in SHA and TTP (Figure 6).

At the outlet of the main catchment (OUT), small rainfall events during wet periods (e.g., events SLRa, LRa and LRb) caused anti-clockwise hysteresis loops while large events after dry periods, indicated by low API_{30}, resulted in clockwise loops indicative of a greater contribution of event water (Evans & Davies, 1998). As observed in the TTP and SHA subcatchments, most rainfall events led to dilution of the NO_3-N

concentration. This indicates that similar flow paths and NO_3-N sources control NO_3-N export in the main catchment, probably as a consequence of the dominance and proximity of these land use types to the outlet of the main catchment (Carey et al., 2014).

4.3. Hot Moments

A large peak in NO_3-N concentrations was observed at the beginning of the rainy season in 2015 in NF and TTP. This could be caused by rapid mineralization of organic matter and a more active, developing microbial community after rewetting of dry soil (Birch, 1964) or accumulation of NO_3-N in the topsoil during the dry season (Kiese et al., 2003). Rapid onset of mineralization and nitrification with rewetting of soils has been observed at several sites in East Africa (Semb & Robinson, 1969) and elsewhere in the tropics (Borken & Matzner, 2004; Butterbach-Bahl et al., 2004). Alternatively, accumulation of inorganic N from decomposition of organic material could occur during a dry spell as a consequence of decreased uptake by primary producers due to water stress (Borken & Matzner, 2004; Wong & Nortcliff, 1995). Thus, first rains after a prolonged dry period can cause a flush of the accumulated NO_3-N into the stream. Quick depletion of this source means that such peaks are only observed at the start of the rainy season with rewetting of soils. Atmospheric N deposition during the dry season could also contribute to NO_3-N accumulation, as observed in a dry catchment in California, USA (Homyak et al., 2014), but N deposition is low in the study area at 2.25 kg ha^{-1} yr^{-1} (Zhou et al., 2014). Nevertheless, similar peaks in NO_3-N export were observed in the transition from dry to wet soils through its effect on microbial N-processing (Homyak et al., 2014). Although these peaks are important hot moments for NO_3-N concentrations, increasing the concentration in the NF subcatchment up to 4 times, their contribution to total annual NO_3-N export was small, due to the low discharge at the end of the dry season. The absence of similar peaks at the start of the rainy season in 2016 suggests that prolonged dry periods are necessary for such flushing events to occur, which is in line with the concept that a combination of a sufficient supply of reactants and suitable environmental conditions are required for this phenomenon to occur (Bernhardt et al., 2017). Nevertheless, the nature of hot moments is that they are difficult to predict.

4.4. NO_3-N Loads

The increased NO_3-N loading in agricultural compared to forested subcatchments in this study, has also been observed in a study comparing 20 tropical catchments in Brazil, where agricultural catchments exported on average 10 times more NO_3-N than natural vegetation catchments (Gücker et al., 2016). Annual loads for NF fall within the range of loads observed in other forests in the tropics (0.02–6.1 kg N ha^{-1} yr^{-1}; supporting information Table S4). The large range of loads obtained from different studies are likely caused by the high variability between tropical catchments, whereby differences in precipitation amount and patterns, hydrological response, temperature, soils, vegetation and topography will result in different flow paths, timing and magnitude of NO_3-N export.

Loads for the SHA and TTP subcatchments are much lower than those observed in agricultural catchments that were converted more than 10 years ago in western Kenya, while a catchment 5 years after conversion had a lower annual NO_3-N load (Recha et al., 2013). The latter did not receive any fertilizer input (Recha et al., 2013), which probably resulted in lower NO_3-N export. Recha et al. (2013) attributed the high NO_3-N load of the older catchments to increased mineralization of soil organic matter, higher population density and higher fertilizer inputs (40 kg N ha^{-1}), which are lower than fertilizer inputs in TTP. However, soils in the study area of Recha et al. (2013) had a higher sand content and pH, which could have increased NO_3-N leaching (Gaines & Gaines, 1994; Sharpley, 1991). In our study, differences in annual NO_3-N exports are most likely related to fertilizer inputs in the agricultural catchments. Although part of the added fertilizer (less than 20 kg N ha^{-1} yr^{-1}, mainly as organic fertilizer in SHA and 150–250 kg N ha^{-1} yr^{-1} predominantly synthetic fertilizer in TTP) is removed through harvesting of crops in SHA and continuous harvesting of young tea leaves in TTP, excess N inputs will be lost through surface runoff, leaching, microbial uptake and as gaseous losses (Figure 6; Arias-Navarro et al., 2017; Mitchell et al., 2009).

Forest cover loss results on average in an increase of annual specific discharge or water yield, the magnitude depending on the amount of forest cover loss (Bosch & Hewlett, 1982; Brown et al., 2005). However, these reviews also show there is a large variability in the change in specific discharge as response to deforestation. In addition to deforestation extent, local climate, soils, topography and geology play an important role. In our case, specific discharge was smaller in SHA than in the other subcatchments, which could be

explained by the 14–28% lower annual precipitation than in NF and TTP. Precipitation in the Mau Forest area generally decreases to the northeast and south of the forest (Williams, 1991) and SHA could be less influenced by thunderstorms originating from Lake Victoria in the west than NF and TTP (Krhoda, 1988). Consequently, in addition to differences in fertilizer inputs and N cycling between the three subcatchments, annual NO_3-N loads in our study are presumably affected by differences in annual specific discharge, but the difference in specific discharge could be largely a result of variation in annual precipitation rather than primarily an effect of land use.

4.5. Downstream Effects

The mean NO_3-N concentration and annual specific load in 2016 at the main outlet was higher than in NF, but not as high as in TTP. Since NO_3-N concentrations and loads in SHA and TTP seem to depend strongly on the amount of fertilizer input, we conclude that fertilizer application on agricultural land increases NO_3-N concentrations and loads and that values observed at OUT will depend on the overall fertilizer input within the catchment. Despite the small share of commercial tea plantations (11%) to the area of the main catchment, but due to the high fertilizer inputs compared to other land use types, tea plantations contributed 27% of the annual NO_3-N load at the outlet of the main catchment (Table 3). The forest and smallholder agriculture contributed 20 and 53%, respectively. Load estimation based on annual specific load and surface area covered by each land use led to a small overestimation of the annual load calculated with data measured at OUT (470 t N yr^{-1}) of 4.9%, showing that land use is a reasonable predictor for annual load estimation within this tropical catchment.

From these results, one can expect that downstream water bodies, such as Lake Victoria in this case, will receive increased NO_3-N loads as a consequence of past and future land use changes. Evidence suggests that the water quality and ecology of Lake Victoria declined in the last decades as consequence of population and economic growth in the region (Juma et al., 2014; Verschuren et al., 2002). Extrapolating the specific loads of the three subcatchments to the Sondu Basin and assuming that loads do not vary regionally and in-stream N removal is negligible, Lake Victoria would have received 1,729 t N in the form of NO_3-N from the Sondu River in 2016 (Table 3). This is 1.5% of the estimated total annual N input to the lake, while the basin covers 1.8% of the complete Lake Victoria basin (2.7% of terrestrial surface area) (Scheren et al., 2000). Further population growth and agricultural expansion (e.g., conversion of forest to smallholder

Table 3
Annual Load Estimation for the Chemosit and Sondu Basins in Kenya for 2016 and Two Scenarios Based on Changes in Land Use and Fertilizer Use

	Annual specific load[a] (kg N ha^{-1} yr^{-1})	Catchment area (%)	Annual load (t N yr^{-1})	Contribution (%)
Chemosit (1,021 km^2)				
Natural forest (NF)	2.6	37	98	20
Smallholder agriculture (SHA)	4.9	52	260	53
Tea and tree plantations (TTP)	12.0	11	135	27
Total estimated annual load			496	
Sondu (3,452 km^2) – current land use				
Natural forest (NF)	2.6	23	206	12
Smallholder agriculture (SHA)	4.9	68	1,150	66
Tea and tree plantations (TTP)	12.0	9	373	22
Total estimated annual load			1,729	
Sondu (3,452 km^2) – scenario 1: all forest converted to smallholder agriculture				
Natural forest (NF)	2.6	0	0	0
Smallholder agriculture (SHA)	4.9	91	1,539	81
Tea and tree plantations (TTP)	12.0	9	373	19
Total estimated annual load			1,912	
Sondu (3,452 km^2) – scenario 2: same fertilizer use in smallholder agriculture as in tea and tree plantations				
Natural forest (NF)	2.6	23	206	6
Smallholder agriculture (SHA)	12.0	68	2,817	83
Tea and tree plantations (TTP)	12.0	9	373	11
Total estimated annual load			3,396	

[a]Based on annual specific load for land use types calculated from the sub-catchments in this study.

agriculture in scenario 1, Table 3) or intensification of fertilizer use (e.g., same level of fertilizer use in smallholder agriculture as in commercial tea plantations in scenario 2, Table 3) could lead to a 11% and 96% increase in annual N loads from the basin, respectively. This would affect the lake through increased eutrophication. Our annual load estimate is, however, 28% higher than the estimated load of 1,347 t N yr^{-1} from the Sondu basin by Kayombo and Jorgensen (2005). Because our estimate is only based on NO_3-N, the total N load is likely higher, since also other forms of N, such as particulate N, ammonium (NH_4-N), nitrite (NO_2-N) and dissolved organic N (DON) need to be considered. The difference between our load estimate and the value reported by Kayombo and Jorgensen (2005) could also be due to the quality and frequency of collected data and the use of different load estimation methods (Littlewood, 1992; Zamyadi et al., 2007). Also, in-stream NO_3-N transformation and uptake between our subcatchments and the outlet of the Sondu Basin, could change NO_3-N concentrations. The calculated specific loads of our study might differ throughout the whole Sondu basin because of differences in underlying geology and soil type, drier and warmer climate, and changes in topography downstream. However, the data presented here is the first approximation to discharge and NO_3-N dynamics and annual N loads and a good basis for upscaling and calibrating hydrological models.

5. Conclusion

This study presented the first high-resolution data set in East Africa. The 2 years of data from natural forest, smallholder agriculture and commercial tea and tree plantations and the main catchment offer valuable insights in NO_3-N dynamics within a tropical montane region in Kenya, as summarized in Figure 6. Our study does not only quantify how land use change impacts the area under change, but also the ecosystems downstream, as shown with the estimated NO_3-N input from the Sondu River to Lake Victoria. A change from natural forest to agriculture seems to increase NO_3-N yields and the occurrence of surface runoff during storm events, in which could lead to increased erosion rates and sediment loads in rivers. Increased nutrient concentrations as a consequence of fertilization can reduce ecological quality of rivers and lakes and affect aquatic life. The high-resolution data collected in this study shows responses to storm events, the processes behind the different responses and hot moments for NO_3-N export. This study highlights the need for wider application of high-resolution monitoring to better understand catchment functioning through analysis of hysteresis loops and hot moments. Although the use of *in situ* instruments has its own challenges, such as security, power supply and maintenance, continuous development of sensor technology and reduction in costs increasingly enables deployment of such sensors, also in remote areas. This is especially relevant in many tropical regions that are vulnerable to land use and climate change. While there is some similarity in general NO_3-N dynamics between our study catchments and temperate catchments, such as increased NO_3-N concentrations and yields due to fertilizer application, dilution of NO_3-N concentrations during rainfall events and the importance of groundwater as source of NO_3-N, underlying biogeochemical processes, like denitrification and decomposition of organic matter, that strongly depend on climatic factors such as precipitation, soil moisture and temperature, are likely to respond differently in tropical regions, where seasonality is often defined by precipitation rather than temperature differences. Therefore, studies using such high-resolution monitoring systems provide valuable data and information to reduce the current knowledge gap in the understanding of the hydrological functioning of and nutrient fluxes in tropical ecosystems.

Acknowledgments
We would like to thank the Kenya Forest Service (KFS) for supporting the research team to conduct this research in the Mau Forest. This work was partially funded by the CGIAR program on Forest, Trees and Agroforestry led by the Centre for International Forestry Research (CIFOR). We thank the Deutsche Forschungsgemeinschaft DFG (BR2238/23-1), and the Deutsche Gesellschaft für Internationale Zusammenarbeit GIZ (grant 81195001 "Low Cost methods for monitoring water quality to inform upscaling of sustainable water management in forested landscapes in Kenya" and grant 81206682 "The Water Towers of East Africa: policies and practices for enhancing co-benefits from joint forest and water conservation") for generously providing additional support SJ received additional funding from the "ATMO" programme of the Helmholtz Association. We are also grateful for the valuable feedback from the reviewers to improve this manuscript. The raw data are currently available in an online database (http://fb09-pasig.umwelt.uni-giessen.de:8050/wiki/publications) hosted by Justus Liebig University, Giessen, Germany.

References

Abbott, B. W., Baranov, V., Mendoza-Lera, C., Nikolakopoulou, M., Harjung, A., Kolbe, T., et al. (2016). Using multi-tracer inference to move beyond single-catchment ecohydrology. *Earth-Science Reviews*, *160*(Suppl. C), 19–42. https://doi.org/10.1016/j.earscirev.2016.06.014

Alvarez-Cobelas, M., Angeler, D. G., & Sánchez-Carrillo, S. (2008). Export of nitrogen from catchments: A worldwide analysis. *Environmental Pollution*, *156*(2), 261–269. https://doi.org/10.1016/j.envpol.2008.02.016

Arias-Navarro, C., Díaz-Pinés, E., Zuazo, P., Rufino, M. C., Verchot, L., & Butterbach-Bahl, K. (2017). Quantifying the contribution of land use to N_2O, NO and CO_2 fluxes in a montane forest ecosystem of Kenya. *Biogeochemistry*, *134*(1-2), 95–114. https://doi.org/10.1007/s10533-017-0348-3

Aubert, A. H., & Breuer, L. (2016). New seasonal shift in in-stream diurnal nitrate cycles identified by mining high-frequency data. *PLoS ONE*, *11*(4), 1–12. https://doi.org/10.1371/journal.pone.0153138

Aubert, A. H., Thrun, M. C., Breuer, L., & Ultsch, A. (2016). Knowledge discovery from high-frequency stream nitrate concentrations: Hydrology and biology contributions. *Scientific Reports*, *6*. https://doi.org/10.1038/srep31536

Bende-Michl, U., Verburg, K., & Cresswell, H. P. (2013). High-frequency nutrient monitoring to infer seasonal patterns in catchment source availability, mobilisation and delivery. *Environmental Monitoring and Assessment*, *185*(11), 9191–9219. https://doi.org/10.1007/s10661-013-3246-8

Bernhardt, E. S., Blaszczak, J. R., Ficken, C. D., Fork, M. L., Kaiser, K. E., & Seybold, E. C. (2017). Control points in ecosystems: Moving beyond the hot spot hot moment concept. *Ecosystems*, *20*(4), 665–682. https://doi.org/10.1007/s10021-016-0103-y

Biggs, T. W., Dunne, T., & Martinelli, L. A. (2004). Natural controls and human impacts on stream nutrient concentrations in a deforested region of the Brazilian Amazon basin. *Biogeochemistry*, *68*(2), 227–257.

Binge, F. W. (1962). *Geology of the Kericho area* (No. 50). Nairobi, Kenya: Ministry of Commerce, Industry and Communications, Geological Survey of Kenya.

Birch, H. F. (1964). Mineralisation of plant nitrogen following alternate wet and dry conditions. *Plant and Soil*, *20*(1), 43–49.

Blaen, P. J., Khamis, K., Lloyd, C. E. M., Bradley, C., Hannah, D., & Krause, S. (2016). Real-time monitoring of nutrients and dissolved organic matter in rivers: Capturing event dynamics, technological opportunities and future directions. *Science of the Total Environment*, *569–570*(Suppl. C), 647–660. https://doi.org/10.1016/j.scitotenv.2016.06.116

Blanco, A. C., Nadaoka, K., Yamamoto, T., & Kinjo, K. (2010). Dynamic evolution of nutrient discharge under stormflow and baseflow conditions in a coastal agricultural watershed in Ishigaki Island, Okinawa, Japan. *Hydrological Processes*, *24*(18), 2601–2616. https://doi.org/10.1002/hyp.7685

Borken, W., & Matzner, E. (2004). Reappraisal of drying and wetting effects on C and N mineralization and fluxes in soils. *Global Change Biology*, *15*(4), 808–824. https://doi.org/10.1111/j.1365-2486.2008.01681.x

Bosch, J. M., & Hewlett, J. D. (1982). A review of catchment experiments to determine the effect of vegetation changes on water yield and evapotranspiration. *Journal of Hydrology*, *55*, 3–23.

Bowes, M. J., Jarvie, H. P., Halliday, S. J., Skeffington, R. A., Wade, A. J., Loewenthal, M., et al. (2015). Characterising phosphorus and nitrate inputs to a rural river using high-frequency concentration-flow relationships. *Science of the Total Environment*, *511*, 608–620.

Bowes, M. J., Smith, J. T., & Neal, C. (2009). The value of high-resolution nutrient monitoring: A case study of the River Frome, Dorset, UK. *Journal of Hydrology*, *378*(1–2), 82–96. https://doi.org/10.1016/j.jhydrol.2009.09.015

Brown, A. E., Zhang, L., McMahon, T. A., Western, A. W., & Vertessy, R. A. (2005). A review of paired catchment studies for determining changes in water yield resulting from alterations in vegetation. *Journal of Hydrology*, *310*(1–4), 28–61. https://doi.org/10.1016/j.jhydrol.2004.12.010

Bruijnzeel, L. A. (2001). Hydrology of tropical montane cloud forests: A reassessment. *Land Use and Water Resources Research*, *1*, 1.1–1.18.

Burt, T. P. (2003). Monitoring change in hydrological systems. *Science of the Total Environment*, *310*(1–3), 9–16. https://doi.org/10.1016/S0048-9697(02)00618-6

Butterbach-Bahl, K., Kock, M., Willibald, G., Hewlett, B., Buhagiar, S., Papen, H., & Kiese, R. (2004). Temporal variations of fluxes of NO, NO_2, N_2O, CO_2, and CH_4 in a tropical rain forest ecosystem. *Global Biogeochemical Cycles*, *18*, GB3012. https://doi.org/10.1029/2004GB002243

Caraco, N. F., & Cole, J. J. (1999). Human impact on nitrate export: An analysis using major world rivers. *Ambio*, *28*(2), 167–170.

Carey, R. O., Wollheim, W. M., Mulukutla, G. K., & Mineau, M. M. (2014). Characterizing storm-event nitrate fluxes in a fifth order suburbanizing watershed using in situ sensors. *Environmental Science & Technology*, *48*(14), 7756–7765. https://doi.org/10.1021/es500252j

Célleri, R., & Feyen, J. (2009). The hydrology of tropical Andean ecosystems: Importance, knowledge status, and perspectives. *Mountain Research and Development*, *29*(4), 350–355. https://doi.org/10.1659/mrd.00007

Chaves, J., Neill, C., Germer, S., Neto, S. G., Krusche, A. V., Bonilla, A. C., & Elsenbeer, H. (2009). Nitrogen transformations in flowpaths leading from soils to streams in Amazon forest and pasture. *Ecosystems*, *12*(6), 961–972. https://doi.org/10.1007/s10021-009-9270-4

Chiti, T., Díaz-Pinés, E., Butterbach-Bahl, K., Marzaioli, F., & Valentini, R. (2017). Soil organic carbon following degradation and conversion to cypress and tea plantations in a tropical mountain forest in Kenya. *Plant and Soil*, *422*(1-2), 527–539. https://doi.org/10.1007/s11104-017-3489-1

Correa, A., Windhorst, D., Tetzlaff, D., Crespo, P., Celleri, R., Feyen, J., & Breuer, L. (2017). Temporal dynamics in dominant runoff sources and flow paths in the Andean Páramo. *Water Resources Research*, *53*, 5998–6017. https://doi.org/10.1002/2016WR020187

Deegan, L. A., Neill, C., Haupert, C. L., Ballester, M. V. R., Krusche, A. V., Victoria, R. L., et al. (2011). Amazon deforestation alters small stream structure, nitrogen biogeochemistry and connectivity to larger rivers. *Biogeochemistry*, *105*(1–3), 53–74. https://doi.org/10.1007/s10533-010-9540-4

Dupas, R., Jomaa, S., Musolff, A., Borchardt, D., & Rode, M. (2016). Disentangling the influence of hydroclimatic patterns and agricultural management on river nitrate dynamics from sub-hourly to decadal time scales. *Science of the Total Environment*, *571*(Suppl. C), 791–800. https://doi.org/10.1016/j.scitotenv.2016.07.053

Durand, P., Breuer, L., Johnes, P. J., Billen, G., Butturini, A., Pinay, G. et al. (2011). Nitrogen processes in aquatic ecosystems. In Sutton, M. A., et al., (Eds.), *The European Nitrogen Assessment* (pp. 126–146). Cambridge, UK: Cambridge University Press.

Evans, C., & Davies, T. D. (1998). Causes of concentration/discharge hysteresis and its potential as a tool for analysis of episode hydrochemistry. *Water Resources Research*, *34*, 129–137.

Ferrant, S., Laplanche, C., Durbe, G., Probst, A., Dugast, P., Durand, P., et al. (2013). Continuous measurement of nitrate concentration in a highly event-responsive agricultural catchment in south-west of France: Is the gain of information useful?. *Hydrological Processes*, *27*(12), 1751–1763. https://doi.org/10.1002/hyp.9324

Fogle, A. W., Taraba, J. L., & Dinger, J. S. (2003). Mass load estimation errors utilizing grab sampling strategies in a Karst watershed. *Journal of the American Water Resources Association*, *39*(6), 1361–1372.

Gaines, T. P., & Gaines, S. T. (1994). Soil texture effect on nitrate leaching in soil percolates. *Communications in Soil Science and Plant Analysis*, *25*(13–14), 2561–2570. https://doi.org/10.1080/00103629409369207

Goodridge, B. M., & Melack, J. M. (2012). Land use control of stream nitrate concentrations in mountainous coastal California watersheds. *Journal of Geophysical Research*, *117*, G02005. https://doi.org/10.1029/2011JG001833

Gücker, B., Silva, R. C. S., Graeber, D., Monteiro, J. A. F., Brookshire, E. N. J., Chaves, R. C., & Boëchat, I. G. (2016). Dissolved nutrient exports from natural and human-impacted Neotropical catchments. *Global Ecology and Biogeography*, *25*(4), 378–390. https://doi.org/10.1111/geb.12417

Halliday, S. J., Skeffington, R. A., Wade, A. J., Neal, C., Reynolds, B., Norris, D., & Kirchner, J. W. (2013). Upland streamwater nitrate dynamics across decadal to sub-daily timescales: A case study of Plynlimon, Wales. *Biogeosciences*, *10*, 8013–8038.

Halliday, S. J., Wade, A. J., Skeffington, R. A., Neal, C., Reynolds, B., Rowland, P., et al. (2012). An analysis of long-term trends, seasonality and short-term dynamics in water quality data from Plynlimon, Wales. *Science of the Total Environment*, *434*, 186–200.

Harmand, J.-M., Ávilla, H., Oliver, R., Saint-André, L., & Dambrine, E. (2010). The impact of kaolinite and oxi-hydroxides on nitrate adsorption in deep layers of a Costarican Acrisol under coffee cultivation. *Geoderma*, *1158*(3–4), 216–224.

Homyak, P. M., Sickman, J. O., Miller, A. E., Melack, J. M., Meixner, T., & Schimel, J. P. (2014). Assessing nitrogen-saturation in a seasonally dry chaparral watershed: Limitations of traditional indicators of N-saturation. *Ecosystems*, *17*(7), 1286–1305. https://doi.org/10.1007/s10021-014-9792-2

ISRIC. (2007). *Soil and terrain database for Kenya, version 2.0, at scale 1:1 million (KENSOTER)*. Wageningen, the Netherlands: ISRIC - World Soil Information.

Jacobs, S. R., Breuer, L., Butterbach-Bahl, K., Pelster, D. E., & Rufino, M. C. (2017). Land use affects total dissolved nitrogen and nitrate concentrations in tropical montane streams in Kenya. *Science of the Total Environment*, *603–604*, 519–532.

Jennings, D. J. (1971). *Geology of the Molo area* (No. 86). Ministry of Natural Resources, Geological Survey of Kenya.

Juma, D. W., Wang, H., & Li, F. (2014). Impacts of population growth and economic development on water quality of a lake: Case study of Lake Victoria Kenya water. *Environmental Science and Pollution Research*, *21*(8), 5737–5746. https://doi.org/10.1007/s11356-014-2524-5

Kayombo, S., & Jorgensen, S. E. (2005). *Lake Victoria. Experience and lessons learned brief* (pp. 431–446). Kusatsu, Japan: International Lake Environment Committee Foundation.

Kiese, R., Hewlett, B., Graham, A., & Butterbach-Bahl, K. (2003). Seasonal variability of N_2O emissions and CH_4 uptake by tropical rainforest soils of Queensland, Australia. *Global Biogeochemical Cycles*, *17*(2), 1043. https://doi.org/10.1029/2002GB002014

Kinyanjui, M. J. (2011). NDVI-based vegetation monitoring in Mau Forest Complex, Kenya. *African Journal of Ecology*, *49*, 165–174.

Kirchner, J. W., Feng, X., Neal, C., & Robson, A. J. (2004). The fine structure of water-quality dynamics: The (high-frequency) wave of the future. *Hydrological Processes*, *18*(7), 1353–1359. https://doi.org/10.1002/hyp.5537

Krhoda, G. O. (1988). The impact of resource utilization on the hydrology of the Mau Hills Forest in Kenya. *Mountain Research and Development*, *8*(2/3), 193–200.

Lewis, W. M., Melack, J. M., McDowell, W. H., McClain, M., & Richey, J. E. (1999). Nitrogen yields from undisturbed watersheds in the Americas. *Biogeochemistry*, *46*(1–3), 149–162. https://doi.org/10.1007/BF01007577

Leys, C., Ley, C., Klein, O., Bernard, P., & Licata, L. (2013). Detecting outliers: Do not use standard deviation around the mean, use absolute deviations around the median. *Journal of Experimental Social Psychology*, *49*, 764–766.

Li, H., Ma, Y., & Liu, W. (2016). Land use and topography as predictors of nitrogen levels in tropical catchments in Xishuangbanna, SW China. *Environmental Earth Sciences*, *75*(6), 539. https://doi.org/10.1007/s12665-015-5241-6

Lin, T.-C., Shaner, P.-J. L., Wang, L.-J., Shih, Y.-T., Wang, C.-P., Huang, G.-H., & Huang, J.-C. (2015). Effects of mountain tea plantations on nutrient cycling at upstream watersheds. *Hydrology and Earth System Sciences*, *19*(11), 4493–4504. https://doi.org/10.5194/hess-19-4493-2015

Littlewood, I. G. (1992). *Estimating contaminant loads in rivers: A review* (No. 117, p. 81). Wallingford, UK: Institute of Hydrology.

Lloyd, C. E. M., Freer, J. E., Johnes, P. J., & Collins, A. L. (2016a). Technical Note: Testing an improved index for analysing storm discharge–concentration hysteresis. *Hydrology and Earth System Sciences*, *20*(2), 625–632. https://doi.org/10.5194/hess-20-625-2016

Lloyd, C. E. M., Freer, J. E., Johnes, P. J., & Collins, A. L. (2016b). Using hysteresis analysis of high-resolution water quality monitoring data, including uncertainty, to infer controls on nutrient and sediment transfer in catchments. *Science of the Total Environment*, *543*(Part A), 388–404. https://doi.org/10.1016/j.scitotenv.2015.11.028

Lohse, K. A., & Matson, P. (2005). Consequences of nitrogen additions for soil losses from wet tropical forests. *Ecological Applications*, *15*(5), 1629–1648.

McClain, M. E., Boyer, E. W., Dent, C. L., Gergel, S. E., Grimm, N. B., Groffman, P. M., et al. (2003). Biogeochemical hot spots and hot moments at the interface of terrestrial and aquatic ecosystems. *Ecosystems*, *6*(4), 301–312. https://doi.org/10.1007/s10021-003-0161-9

McMillan, H., Freer, J., Pappenberger, F., Krueger, T., & Clark, M. (2010). Impacts of uncertain river flow data on rainfall-runoff model calibration and discharge predictions. *Hydrological Processes*, *24*(10), 1270–1284. https://doi.org/10.1002/hyp.7587

Mitchell, A., Reghenzani, J., Faithful, J., Furnas, M., & Brodie, J. (2009). Relationships between land use and nutrient concentrations in streams draining a "wet-tropics" catchment in northern Australia. *Marine and Freshwater Research*, *60*(11), 1097–1108. https://doi.org/10.1071/MF08330

Mitchell, M. J. (2001). Linkages of nitrate losses in watersheds to hydrological processes. *Hydrological Processes*, *15*(17), 3305–3307. https://doi.org/10.1002/hyp.503

Moatar, F., Abbott, B. W., Minaudo, C., Curie, F., & Pinay, G. (2017). Elemental properties, hydrology, and biology interact to shape concentration-discharge curves for carbon, nutrients, sediment, and major ions. *Water Resources Research*, *53*, 1270–1287. https://doi.org/10.1002/2016WR019635

Moore, R. D. (2004). Introduction to salt dilution gauging for streamflow measurement: Part 1. *Streamline Watershed Management Bulletin*, *7*(4), 20–23.

Musolff, A., Schmidt, C., Selle, B., & Fleckenstein, J. H. (2015). Catchment controls on solute export. *Advances in Water Resources*, *86*(Part A), 133–146. https://doi.org/10.1016/j.advwatres.2015.09.026

Neal, C., Reynolds, B., Rowland, P., Norris, D., Kirchner, J. W., Neal, M., et al. (2012). High-frequency water quality time series in precipitation and streamflow: From fragmentary signals to scientific challenge. *Science of the Total Environment*, *434*, 3–12.

Neill, C., Deegan, L. A., Thomas, S. M., & Cerri, C. C. (2001). Deforestation for pasture alters nitrogen and phosphorus in small Amazonian streams. *Ecological Applications*, *11*(6), 1817–1828. https://doi.org/10.2307/3061098

Owuor, S. O., Butterbach-Bahl, K., Guzha, A. C., Jacobs, S., Merbold, L., Rufino, M. C., et al. (2018). Conversion of natural forest results in a significant degradation of soil hydraulic properties in the highlands of Kenya. *Soil and Tillage Research*, *176*, 36–44.

Pellerin, B. A., Bergamaschi, B. A., Gilliom, R. J., Crawford, C. G., Saraceno, J. F., Frederick, C. P., et al. (2014). Mississippi River nitrate loads form high frequency sensor measurements and regression-based load estimation. *Environmental Science & Technology*, *48*(21), 12612–12619.

Pellerin, B. A., Downing, B. D., Kendall, C., Dahlgreen, R. A., Kraus, T. E. C., Saraceno, J., et al. (2009). Assessing the sources and magnitude of diurnal nitrate variability in the San Joaquin River (California) with an in situ optical nitrate sensor and dual nitrate isotopes. *Freshwater Biology*, *54*(2), 376–387.

Rasiah, V., Armour, J. D., Yamamoto, T., Mahendrarajah, S., & Heiner, D. H. (2003). Nitrate dynamics in shallow groundwater and the potential for transport to off-site water bodies. *Water, Air, and Soil Pollution*, *147*(1–4), 183–202. https://doi.org/10.1023/A:1024529017142

R Core Team. (2015). *R: A language and environment for statistical computing. (Version 3.2.1)*. Vienna, Austria: R Foundation for Statistical Computing. Retrieved from http://www.R-project.org/

Recha, J. W., Lehmann, J., Walter, M. T., Pell, A., Verchot, L., & Johnson, M. (2013). Stream water nutrient and organic carbon exports from tropical headwater catchments at a soil degradation gradient. *Nutrient Cycling in Agroecosystems*, *95*(2), 145–158. https://doi.org/10.1007/s10705-013-9554-0

Ribeiro, K. H., Favaretto, N., Dieckow, J., de Paula Souza, L. C., Minella, J. P. G., de Almeida, L., & Ramos, M. R. (2014). Quality of surface water related to land use: A case study in a catchment with small farms and intensive vegetable crop production in southern Brazil. *Revista Brasileira de Ciência De Solo*, *38*(2), 656–668.

Riskin, S. H., Neill, C., Jankowski, K., Krusche, A. V., McHorney, R., Elsenbeer, H., et al. (2017). Solute and sediment export from Amazon forest and soybean headwater streams. *Ecological Applications*, *27*(1), 193–207. https://doi.org/10.1002/eap.1428

Rode, M., Wade, A. J., Cohen, M. J., Hensley, R. T., Bowes, M. J., Kirchner, J. W., et al. (2016). Sensors in the stream: The high-frequency wave of the present. *Environmental Science & Technology*, *50*(19), 10297–10307. https://doi.org/10.1021/acs.est.6b02155

Rozemeijer, J. C., van der Velde, Y., van Geer, F. C., de Rooij, G. H., Torfs, P. J. J. F., & Broers, H. P. (2010). Improving load estimates for NO_3 and P in surface waters by characterizing the concentration response to rainfall events. *Environmental Science & Technology*, *44*(16), 6305–6312. https://doi.org/10.1021/es101252e

Saunders, T. J., McClain, M. E., & Llerena, C. A. (2006). The biogeochemistry of dissolved nitrogen, phosphorus, and organic carbon along terrestrial-aquatic flowpaths of a montane headwater catchment in the Peruvian Amazon. *Hydrological Processes*, *20*(12), 2549–2562. https://doi.org/10.1002/hyp.6215

Scheren, P. A. G. M., Zanting, H. A., & Lemmens, A. M. C. (2000). Estimation of water pollution sources in Lake Victoria, East Africa: Application and elaboration of the rapid assessment methodology. *Journal of Environmental Management*, *58*(4), 235–248. https://doi.org/10.1006/jema.2000.0322

Semb, G., & Robinson, J. B. D. (1969). The natural nitrogen flush in different arable soils and climates in East Africa. *East African Agricultural and Forestry Journal*, *34*(3), 350–370. https://doi.org/10.1080/00128325.1969.11662315

Sharpley, A. N. (1991). Effect of soil pH on cation and anion solubility. *Communications in Soil Science and Plant Analysis*, *22*(9–10), 827–841. https://doi.org/10.1080/00103629109368457

Sherson, L. R., Van Horn, D. J., Gomez-Velez, J. D., Crossey, L. J., & Dahm, C. N. (2015). Nutrient dynamics in an alpine headwater stream: Use of continuous water quality sensors to examine responses to wildfire and precipitation events. *Hydrological Processes*, *29*, 3193–3207.

Soares, M. R., Alleoni, L. R. F., Vidal-Torrado, P., & Cooper, M. (2005). Mineralogy and ion exchange properties of the particle size fractions of some Brazilian soils in tropical humid areas. *Geoderma*, *125*(3–4), 355–367.

Swart, R. (2016). *Monitoring 40 years of land use change in the Mau Forest Complex, Kenya. A land use change driver analysis* (MSc thesis). Wageningen, the Netherlands: Wageningen University.

UNEP, Kenya Wildlife Service, Kenya Forest Working Group, & Ewaso Ngiro South Development Authority. (2008). *Mau complex under siege. Values and threats* Nairobi, Kenya: UNEP.

Van Herpe, Y., & Troch, P. A. (2000). Spatial and temporal variations in surface water nitrate concentrations in a mixed land use catchment under humid temperate climatic conditions. *Hydrological Processes*, *14*(14), 2439–2455. https://doi.org/10.1002/1099-1085(20001015)14:14<2439::AID-HYP105>3.0.CO;2-H

Verschuren, D., Johnson, T. C., Kling, H. J., Edgington, D. N., Leavitt, P. R., Brown, E. T., et al. (2002). History and timing of human impact on Lake Victoria, East Africa. *Proceedings: Biological Sciences*, *269*(1488), 289–294.

Waterloo, M. J., Oliveira, S. M., Drucker, D. P., Nobre, A. D., Cuartas, L. A., Hodnett, M. G., et al. (2006). Export of organic carbon in run-off from an Amazonian rainforest blackwater catchment. *Hydrological Processes*, *20*(12), 2581–2597. https://doi.org/10.1002/hyp.6217

Williams, L. A. J. (1991). *Geology of the Mau area* (No. 96). Ministry of Environment and Natural Resources, Mines and Geological Department.

Williams, M. R., & Melack, J. M. (1997). Solute export from forested and partially deforested catchments in the Central Amazon. *Biogeochemistry*, *38*(1), 67–102.

Wong, M. T. F., & Nortcliff, S. (1995). Seasonal fluctuations of native available N and soil management implications. *Fertilizer Research*, *42*(1–3), 13–26. https://doi.org/10.1007/BF00750496

Zamyadi, A., Gallichand, J., & Duchemin, M. (2007). Comparison of methods for estimating sediment and nitrogen loads from a small agricultural watershed. *Canadian Biosystems Engineering*, *49*, 27–36.

Zhou, M., Brandt, P., Pelster, D., Rufino, M. C., Robinson, T., & Butterbach-Bahl, K. (2014). Regional nitrogen budget of the Lake Victoria Basin, East Africa: Syntheses, uncertainties and perspectives. *Environmental Research Letters*, *9*(10), 105009. https://doi.org/10.1088/1748-9326/9/10/105009

Zuijdgeest, A., Baumgartner, S., & Wehrli, B. (2016). Hysteresis effects in organic matter turnover in a tropical floodplain during a flood cycle. *Biogeochemistry*, *131*(1–2), 49–63. https://doi.org/10.1007/s10533-016-0263-z